


 Cite this: *RSC Adv.*, 2024, 14, 2447

# Divalent manganese stimulates the removal of nitrate by anaerobic sludge

 Zhaojie Jiang,<sup>ID</sup> <sup>b</sup> Xuejiao Huang,<sup>\*ad</sup> Shuangfei Wang,<sup>c</sup> Jianhua Xiong,<sup>bd</sup> Chunmin Xie<sup>d</sup> and Yongli Chen<sup>d</sup>

This study investigated the effect of different concentrations of  $Mn^{2+}$  on the removal of nitrate by anaerobic sludge and changes in the microbial communities through batch experiments. The results showed that the addition of  $Mn^{2+}$  promoted nitrate removal by anaerobic sludge; the nitrate was completely removed within 6 d in the treatment group with  $>5$  mM  $Mn^{2+}$ . With the increase in  $Mn^{2+}$ , the concentration of nitrite and nitrous oxide increased in the first 4 d and then decreased to 0  $\mu M$  after 8 d of incubation. The increasing tendency of ammonium increased firstly and then decreased with the addition of  $Mn^{2+}$  compared to A. Moreover, the  $Mn^{2+}$  removal efficiency gradually decreased with the increase of  $Mn^{2+}$  concentration. The changes of microflora structure in sludge before and after adding  $Mn^{2+}$  were analyzed, and the results revealed that the microbial communities in the sludge may have evolved towards an energy-efficient association of short-cut nitrification, denitrification, and anaerobic ammonia oxidation after adding  $Mn^{2+}$ .  $Mn^{2+}$  stimulated the removal of nitrate by anaerobic sludge mainly by promoting the growth of *PHOS-HE36*.

Received 18th October 2023

Accepted 7th January 2024

DOI: 10.1039/d3ra07088c

[rsc.li/rsc-advances](https://rsc.li/rsc-advances)

## 1. Introduction

With the acceleration of industrialization and urbanization, and the widespread use of agricultural fertilizers,  $NO_3^-$ -N pollution of water bodies has become a prominent environmental problem.<sup>1,2</sup>  $NO_3^-$  is a highly soluble, widespread pollutant in aquatic environments, and it is widely found in surface water, groundwater, and wastewater.<sup>3,4</sup> Groundwater, which is an important water resource, is currently the main source of drinking and industrial water in China,<sup>5</sup> and  $NO_3^-$ -N contamination is a serious threat to drinking water safety. High levels of  $NO_3^-$ -N in groundwater pose a threat to human health (e.g., methemoglobinemia).<sup>6</sup> Therefore, there is an urgent need to reduce  $NO_3^-$ -N concentrations in groundwater. Conventional heterotrophic denitrification techniques require the addition of an external organic carbon source and regulation of the amount of carbon to prevent nitrite accumulation or high organic matter contents in the wastewater, which is unsustainable on both an economic and environmental scale. In recent decades, as energy and environmental issues have

become more prominent, organic waste has been used as an external organic carbon source to satisfy the needs of the heterotrophic denitrification process. For example, short-chain fatty acids, waste leachate, and hydrolyzed primary sludge have been successfully applied for denitrification, maintaining a balance in waste management as well the efficient use of nitrogen removal properties.<sup>7</sup> Anaerobic digestion (AD) is a promising biomass energy conversion technology that has been widely used in integrated treatments of livestock manure, sewage sludge, and food waste.<sup>8</sup> Some scholars have developed an anaerobic simultaneous denitrification and methanogenesis process based on AD for  $NO_3^-$ -N removal without the need for additional nitrogen removal equipment or organic carbon sources.<sup>9</sup>

AD includes hydrolysis, acidification, and methanogenesis steps. Nitrogen conversion during AD includes microbial assimilation, ammonification, denitrification, and anaerobic ammonia oxidation. These reactions rely mainly on anaerobic microorganisms. Trace metal elements are important sources of microbial nutrients that are crucial for the synthesis and activity of enzymes in the AD process. These microbial nutrients promote the decomposition of organic matter and enhance the production of biogas and methane ( $CH_4$ ).<sup>10</sup> Low concentrations of essential metals (e.g., Fe, Cu, Mn, Zn, and Co) can stimulate biological systems.<sup>11</sup> However, above a certain threshold, they can affect or even inhibit microbial growth and metabolic activity.<sup>12</sup>

Excess  $NO_3^-$ -N in natural groundwater bodies is often accompanied by high concentrations of  $Mn^{2+}$ .<sup>13</sup> Coupled with

<sup>a</sup>Guangxi Key Laboratory of Agro-Environment and Agro-Product Safety, College of Agriculture, Guangxi University, Nanning, Guangxi 530004. E-mail: hxuejiao0412@sina.com; Tel: +86 18577976592

<sup>b</sup>School of Resources, Environment and Materials, Guangxi University, Nanning 530004, China

<sup>c</sup>College of Light Industry and Food Engineering, Guangxi University, Nanning, Guangxi 530004, China

<sup>d</sup>Guangxi Bossco Environmental Protection Technology Co., Ltd., Nanning 530007, Guangxi, China



microorganisms,  $\text{Mn}^{2+}$  and  $\text{Mn}^{4+}$  can act as reducing and oxidizing agents in oceans, soils, continental shelves, and sediments to facilitate the formation of biochemical interactions. Moreover, the manganese redox cycle can efficiently augment microbial metabolic processes. Specifically,  $\text{Mn}^{2+}$  acts as a reductant to provide an electron donor for anaerobic denitrification reactions, including  $\text{Mn}^{2+}$ -driven denitrification and  $\text{Mn}^{2+}$  oxidation combined with nitrification.<sup>14</sup> He *et al.*<sup>15</sup> found that  $0.5 \text{ mg L}^{-1}$  significantly stimulated denitrification by *Arthrobacter arilaitensis* Y-10. Liu *et al.*<sup>16</sup> revealed that under sustained manganese-humic acid complex domestication conditions, the sludge microbial community may have evolved into an energy-efficient consortium of short-cut nitrification, denitrification, and anaerobic ammonia oxidation to achieve excellent ammonium removal. However, little attention has been paid to the influence of  $\text{Mn}^{2+}$  on the removal of  $\text{NO}_3^-$ -N by anaerobic sludge.

Therefore, this study focused on the effect of  $\text{Mn}^{2+}$  on the  $\text{NO}_3^-$ -N removal capacity of anaerobic sludge. The relationship between  $\text{Mn}^{2+}$  and microbial community structure was also analyzed. The results provide a reference for the application of anaerobic sludge to the  $\text{Mn}^{2+}$ -containing nitrate wastewater.

## 2. Results and discussion

### 2.1. Effect of $\text{Mn}^{2+}$ on nitrogen transformation in anaerobic sludge

The effect of  $\text{Mn}^{2+}$  on  $\text{NO}_3^-$ -N removal is shown in Fig. 1a. In the initial stage (0–2 d), the  $\text{NO}_3^-$ -N removal rate of the treatment groups was in the order of  $A > C > B > D > E > F$ , and the  $\text{NO}_3^-$ -N removal rate of the control group was significantly higher than that of the other treatment groups. This may have occurred because the addition of  $\text{Mn}^{2+}$  hindered the adaptation of microorganisms involved in denitrification, and the

microorganisms were in a stagnant period of growth and metabolism, which decelerated the  $\text{NO}_3^-$ -N removal rate. With an increase in time, the microorganisms adapted to the environment and started to develop, the  $\text{NO}_3^-$ -N removal rates of the treatment groups exceeded that of the control group, and  $\text{NO}_3^-$ -N was completely removed within 6 d in the treatment group with  $>5 \text{ mM Mn}^{2+}$ . The average  $\text{NO}_3^-$ -N removal rate of groups with  $>10 \text{ mM Mn}^{2+}$  increased by 0.404, 0.429, and  $0.697 \text{ mM d}^{-1}$  after 2–4 d compared with the initial stage, and the  $\text{NO}_3^-$ -N was completely removed within 8 d, which indicated that the addition of  $\text{Mn}^{2+}$  promoted  $\text{NO}_3^-$ -N removal. This might be because there are manganese-oxidizing bacteria in the anaerobic sludge and they oxidised  $\text{Mn}^{2+}$  to form  $\text{Bio-MnOx}$  to stimulate nitrogen removal.<sup>7,16–18</sup> The  $\text{NH}_4^+$ -N concentration of each treatment group increased continuously with time, first, at a fast rate and then at a slower rate, followed by a levelled period (Fig. 1b). This may have occurred because of the higher degree of protein hydrolysis at the early reaction stage. The faster growth of  $\text{NH}_4^+$ -N and the later stage of the sludge entering the methanogenic stage was coupled with the depletion of nutrients, which reduced the protein content and decelerated the  $\text{NH}_4^+$ -N growth.<sup>19</sup> With the increase in  $\text{Mn}^{2+}$ , the  $\text{NH}_4^+$ -N content decreased and then increased, and the lowest  $\text{NH}_4^+$ -N concentration was observed in the group with the addition of  $10 \text{ mM Mn}^{2+}$ . This could be attributed to the fact that as the  $\text{Mn}^{2+}$  content increased, the extreme environment enhanced sludge hydrolysis, which led to an increase in the production of  $\text{NH}_4^+$ -N. Moreover, the utilization of  $\text{NH}_4^+$ -N might be affected by the bacterial activity of ammonia oxidation and the nitrate anisotropic reduction to ammonia (DNRA).  $\text{NO}_2^-$ -N and  $\text{N}_2\text{O}$  are common intermediates in denitrification, and their production is shown in Fig. 1c and d. At different stages, both  $\text{NO}_2^-$ -N and  $\text{N}_2\text{O}$  accumulated, and their concentrations increased and then decreased to  $0 \text{ mg L}^{-1}$ . The groups treated with 1, 5, and  $10 \text{ mM Mn}^{2+}$  presented higher accumulation of  $\text{NO}_2^-$ -N on day 2, and the group treated with  $5 \text{ mM Mn}^{2+}$  presented the highest accumulation. However, there was no accumulation in any of the treatment groups after 4 d. Previous studies have shown that high  $\text{Mn}^{2+}$  concentrations under pure bacterial conditions can lead to higher  $\text{NO}_2^-$ -N accumulation.<sup>13</sup> However, the  $\text{NO}_2^-$ -N produced in this study did not accumulate. The following processes may have occurred: (1) complete denitrification; (2) anaerobic ammonia oxidation with  $\text{NH}_4^+$ -N from sludge hydrolysis to produce  $\text{N}_2$ ; (3) production of  $\text{NH}_4^+$ -N via the DNRA pathway. The groups treated with 10, 15, and  $20 \text{ mM Mn}^{2+}$  showed detectable accumulation of  $\text{N}_2\text{O}$  in the first 8 d, with production in the order of  $F > E > D$ . However, there was no  $\text{N}_2\text{O}$  accumulation in the other treatment groups, probably because the increase in  $\text{Mn}^{2+}$  addition stimulated denitrification and inhibited anaerobic ammonia oxidation.

### 2.2. Effect of $\text{Mn}^{2+}$ on TN removal and $\text{Mn}^{2+}$ changes in anaerobic sludge

The TN concentration and pH changes in the supernatant after 12 d are shown in Fig. 2a. Owing to the low organic nitrogen

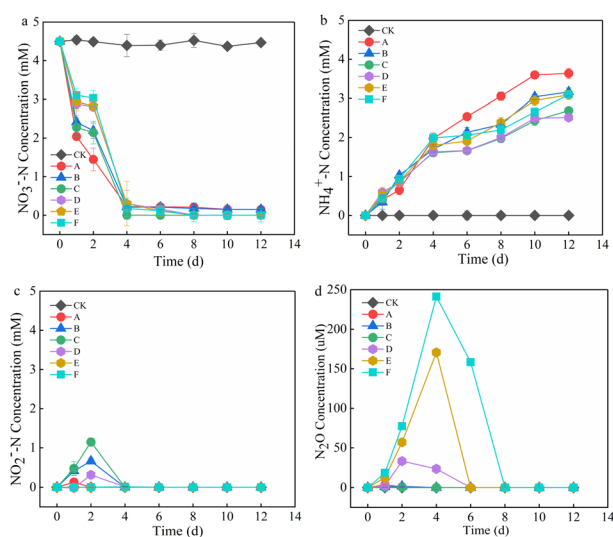


Fig. 1 Variation of (a)  $\text{NO}_3^-$ -N, (b)  $\text{NH}_4^+$ -N, (c)  $\text{NO}_2^-$ -N, and (d)  $\text{N}_2\text{O}$  in the supernatant. CK is the blank control, whereas A, B, C, D, E, and F represent the groups treated with 0, 1, 5, 10, 15, and  $20 \text{ mM Mn}^{2+}$ , respectively.



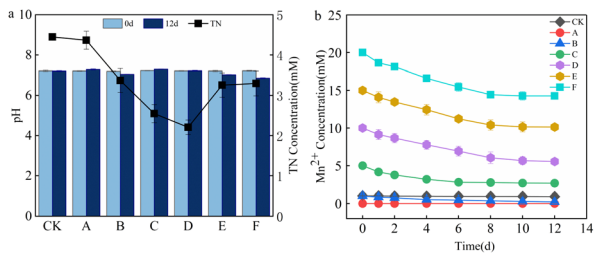
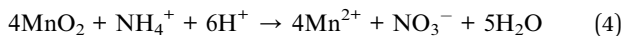
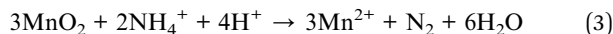
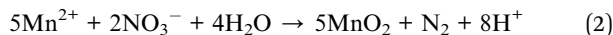


Fig. 2 Changes in supernatant (a) pH and TN concentration, and (b)  $\text{Mn}^{2+}$  concentration from day 0 to 12. CK is the blank control, whereas A, B, C, D, E, and F represent the groups treated with 0, 1, 5, 10, 15, and 20 mM of  $\text{Mn}^{2+}$ , respectively.

content in the supernatant,  $\text{NO}_3^-$ -N was totally removed, and there was no accumulation of  $\text{NO}_2^-$ -N. The supernatant TN concentration in the system was nearly the same as the  $\text{NH}_4^+$ -N accumulation. The supernatant TN removal rates of groups A to F were 2.95, 25.13, 43.42, 50.96, 27.66, and 26.76%, respectively. As the  $\text{Mn}^{2+}$  content increased, the TN removal first increased and then decreased. The pH of each treatment group measured on day 12 did not change significantly, which indicated that the sludge AD system was stable. During the AD, the degradation of nitrogenous organic matter increased the alkalinity of the system, and the production and dissolution of  $\text{CO}_2$  generated carbonic acid, which formed a buffer system. This buffer balanced the small-scale fluctuation of the acid base.<sup>20</sup> Fig. 2b shows the variation in  $\text{Mn}^{2+}$  concentration. According to previous studies,  $\text{Mn}^{2+}$  might be involved in the following processes.<sup>21–23</sup>



$\text{Mn}^{2+}$  can act as an electron donor for denitrification and be oxidized. Ammonia-oxidizing bacteria can reduce  $\text{MnO}_2$  to  $\text{Mn}^{2+}$  under anoxic manganese-rich conditions.<sup>17,22</sup>  $\text{Mn}^{2+}$  oxidation usually occurs in environments rich in organic compounds and microorganisms, and  $\text{Mn}^{2+}$  acts as a reducing agent in anaerobic oxidation reactions, supplying electrons to a variety of biochemical processes, including denitrification and anaerobic photosynthesis. The anaerobic sludge added to each treatment group contained organic matter and microorganisms. Therefore, the  $\text{Mn}^{2+}$  concentration decreased in all treatment groups. The gradual decrease in  $\text{Mn}^{2+}$  removal efficiency with increasing  $\text{Mn}^{2+}$  concentration might be attributed to the fact that the microorganisms have a higher activity and can better utilize  $\text{Mn}^{2+}$  for denitrification in an environment with low  $\text{Mn}^{2+}$  concentration. Alternatively, more  $\text{MnO}_2$  was reduced to  $\text{Mn}^{2+}$  as the activity of ammonia-oxidizing bacteria increased with increasing  $\text{Mn}^{2+}$  concentration. The  $\text{Mn}^{2+}$

concentration remained almost unchanged in the CK group, the kinetics of abiotic Mn oxidation were essentially low, and it has been shown that abiotic manganese oxidation does not occur at pH 7.2,<sup>24</sup> so the  $\text{Mn}^{2+}$  concentration in the CK group remains constant.

### 2.3. Microbial community changes under different $\text{Mn}^{2+}$ concentrations

**2.3.1. Similarities and differences in the microbial community.** Alpha diversity is an indicator of species richness, diversity, and evenness in homogeneous habitats. Richness was characterized by Chao1 and observed species indices. Diversity, evolution-based diversity, and evenness were characterized by Simpson's, Faith's PD, and Pielou's evenness indexes, respectively.<sup>25</sup> As shown in Fig. 3a, the species richness and evolutionary diversity of the treatment groups upon the addition of  $<15$  mM  $\text{Mn}^{2+}$  increased and then decreased with the addition of  $\text{Mn}^{2+}$ . The group treated with 15 mM  $\text{Mn}^{2+}$  was the most species-rich. According to the Simpson's index, the species diversity and evenness decreased as the  $\text{Mn}^{2+}$  concentration increased. This probably because that the high  $\text{Mn}^{2+}$  concentration kills intolerant species. The Venn diagram shows the number of shared and unique species among the samples, and it reflects the similarities and differences in microbial composition. As shown in Fig. 3b, the number of OUTs shared by the six treatment groups was 715, which represents a relatively small percentage, thereby indicating that the microbial composition of the treatment groups differed greatly.

**2.3.2. Structural composition of microbial communities.** The bacterial communities of the different treatments after 12 d of incubation were analysed using high-throughput sequencing, and the differences in microbial communities of different treatment groups were analysed at the phylum and genus levels, as shown in Fig. 4a and b. Proteobacteria,

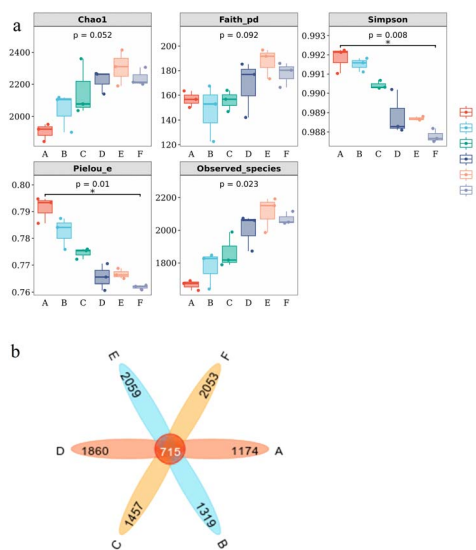


Fig. 3 Alpha index diversity (a) box-line plot and (b) Venn diagram. A, B, C, D, E, and F represent the groups treated with 0, 1, 5, 10, 15, and 20 mM of  $\text{Mn}^{2+}$ , respectively.

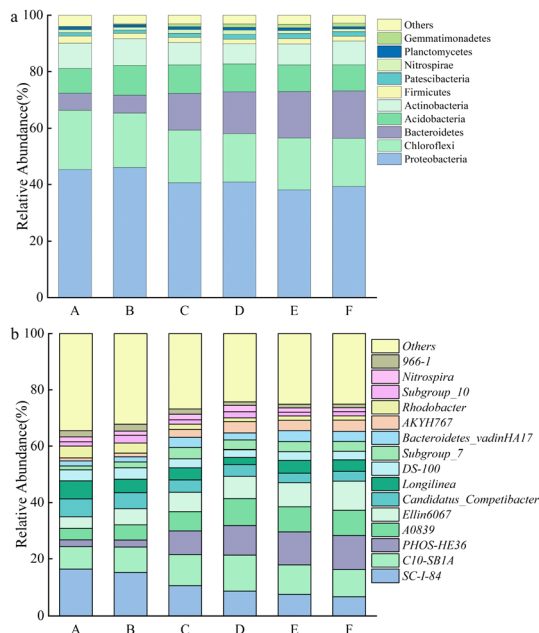


Fig. 4 Relative abundance of bacterial communities at the (a) phylum and (b) genus level. A, B, C, D, E, and F represent the groups treated with 0, 1, 5, 10, 15, and 20 mM of  $Mn^{2+}$ , respectively.

Chloroflexi, Bacteroidetes, Acidobacteria, and Actinobacteria were the dominant phyla in the sludge AD system (Fig. 4a). The highest abundance of Proteobacteria was probably related to its diverse substrate utilization and environmental adaptation. Proteobacteria, Bacteroidetes, and Acidobacteria are closely related to the nitrogen cycle. Moreover, Proteobacteria and Chloroflexi are completely denitrifying microorganisms, which are essential in the denitrification process.<sup>26,27</sup> The relative abundances of Proteobacteria and Chloroflexi had little change with the increase in  $Mn^{2+}$ , while the abundance of Bacteroidetes increased significantly with the  $Mn^{2+}$  concentration increased from 0–5 mM and then gradually increased in the  $Mn^{2+}$  concentration of 5–20 mM. The Anabaena phylum is the dominant bacteria in the hydrolysis and acidification stages of anaerobic systems involved in the production of acetic acid and propionic acid,<sup>28</sup> and its relative abundance gradually increased with the increase in  $Mn^{2+}$  concentration, which promoted sludge hydrolysis.

At the genus level, the bacteria associated with denitrification in the top 15 dominant genera included *SC-I-84*, *C10-SB1A*, *PHOS-HE36*, *Ellin6067*, *Candidatus\_Competibacter*, *Subgroup\_10*, and *Nitrospira*.<sup>29–31</sup> *SC-I-84* is known as an anaerobic ammonia-oxidizing bacteria.<sup>32</sup> As the  $Mn^{2+}$  concentration increased, the relative abundance of *SC-I-84* gradually decreased, and anaerobic ammonia oxidation gradually weakened (Fig. 4b). *C10-SB1A* is considered a DNRA bacteria,<sup>31</sup> and its relative abundance first increased and then decreased with the increase in  $Mn^{2+}$  concentration, and reached the maximum in the group with 10 mM  $Mn^{2+}$  treatment. The phenomenon revealed that the DNRA in the system was first enhanced and then weakened. Some studies have shown that *PHOS-HE36* and *Subgroup\_10* are

denitrifying bacteria,<sup>33</sup> and the relative abundance of *PHOS-HE36* gradually increased as the  $Mn^{2+}$  concentration increased, indicating the gradually strengthening of denitrification. *Candidatus\_Competibacter* are glycogen-accumulating organisms (GAOs) that can store nutrients. GAOs are functional bacteria in the process of endogenous denitrification of treated municipal wastewater, which can convert  $NO_3^- - N$  and  $NO_2^- - N$  to  $N_2$ .<sup>31</sup> As the  $Mn^{2+}$  concentration increased, the relative abundance of *Candidatus\_Competibacter* gradually decreased, and endogenous denitrification weakened. *Ellin6067* is an ammonia-oxidizing bacteria (AOB), which oxidizes ammonia to nitrite. AOB are autotrophic bacteria that oxidize  $NH_4^+ - N$  for energy by using  $CO_2$  as a carbon source.<sup>34</sup> *Nitrospira* is a complete ammonia-oxidizing bacteria (comammox), whose genome contains a complete genetic material encoding the full process of ammonia oxidation and nitrite oxidation, and they can directly oxidize  $NH_4^+$  to  $NO_3^-$ .<sup>35</sup> As the  $Mn^{2+}$  concentration increased, the relative abundance of *Ellin6067* gradually increased, which promoted the conversion of  $NH_4^+ - N$  to  $NO_2^- - N$ ; whereas the relative abundance of *Nitrospira* first increased and then decreased. The relative abundance of the group treated with 10 mM  $Mn^{2+}$  was the largest, and *Nitrospira* presented the highest utilization rate of  $NH_4^+ - N$ . In summary, the removal of  $NO_3^- - N$  occurred through the combined action of denitrification, ammonia oxidation, and DNRA. As the  $Mn^{2+}$  concentration increased, denitrification was gradually enhanced, anaerobic ammonia oxidation was slowly weakened, and DNRA was first enhanced and then weakened, microbial communities may have evolved towards an energy-efficient association of short-cut nitrification, denitrification, and anaerobic ammonia oxidation. The concentration of  $NH_4^+ - N$  accumulated in the supernatant decreased and then increased with increasing  $Mn^{2+}$  concentration under the combined action of hydrolysing bacteria, AOB, comammox, and DNRA.

**2.3.3. Canonical correlation analysis (CCA) of denitrification-associated genus-level microorganisms.** The CCA of denitrification microbial communities associated with  $Mn^{2+}$  and nitrate reduction rate (NRR) at the genus level is showed in Fig. 5. The eigenvalues of the two axes were 92.69 and

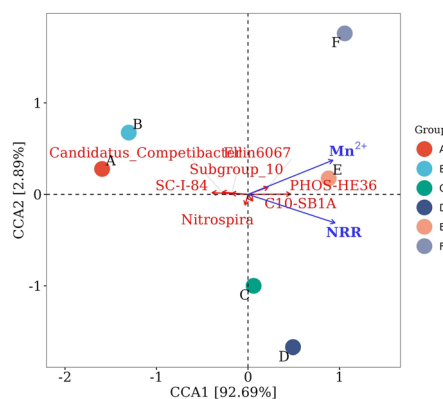


Fig. 5 Microbial CCA related to denitrification at the genus level. A, B, C, D, E, and F represent the groups treated with 0, 1, 5, 10, 15, and 20 mM of  $Mn^{2+}$ , respectively.



2.89%, and both  $Mn^{2+}$  and NRR were strongly correlated with axis 1. The microbial community structure was more similar in treatment groups A and B, with significant differences from the other groups. The addition of  $>5$  mM  $Mn^{2+}$  substantially affected the composition of the microbial community structure. The relative abundance of *SC-I-84* was significantly negatively correlated with  $Mn^{2+}$  concentration, which indicated that the addition of  $Mn^{2+}$  inhibited the growth of *SC-I-84* and that anaerobic ammonia oxidation gradually weakened with the addition of  $Mn^{2+}$ . NRR was positively correlated with initial  $Mn^{2+}$  concentration. Moreover, the relative abundances of *C10-SB1A*, *PHOS-HE36*, and *Ellin6067* were positively correlated with NRR and  $Mn^{2+}$  concentrations. *PHOS-HE36* presented the greatest effect on  $NO_3^-$ -N removal, which suggested that the addition of  $Mn^{2+}$  promoted the growth of *PHOS-HE36*, which in turn promoted  $NO_3^-$ -N removal. AOB can reduce  $MnO_2$  to  $Mn^{2+}$  in anoxic manganese-rich environments.<sup>18</sup> In this study, *Ellin6067*, an AOB, which was significantly positively correlated with  $Mn^{2+}$  concentrations (Fig. 5). The result indicated that *Ellin6067* can tolerate a high concentration of  $Mn^{2+}$  and is hypothesized to reduce  $MnO_2$  to  $Mn^{2+}$ .

The wastewater used in this study is synthetic groundwater formulated according to the actual situation, which cannot completely simulate the actual situation. In the future, pilot-scale experiments using actual wastewater would be conducted. Moreover, the effect of  $Mn^{2+}$  on  $NO_3^-$ -N removal by anaerobic sludge was investigated in this study. The results of the study are closely related to the microorganisms in the sludge, and may vary depending on the composition of the microbial community in different sludges.

### 3. Conclusions

Denitrification, anaerobic ammonia oxidation, and DNRA ensured the removal effect of  $NO_3^-$ -N in anaerobic sludge. The addition of  $Mn^{2+}$  promoted the removal efficiency of  $NO_3^-$ -N and TN. The fastest  $NO_3^-$ -N removal was obtained by the group treated with 5 mM  $Mn^{2+}$ , and the best TN removal was found by the group addition with 10 mM  $Mn^{2+}$ . The addition of  $Mn^{2+}$  contributed to the removal of  $NO_3^-$ -N mainly by promoting the growth of the genus *PHOS-HE36* in the anaerobic sludge.

### 4. Experimental

#### 4.1. Domestication of anaerobic sludge

Sludge was obtained from the Xingchang Wastewater Treatment Plant, Zhejiang, China. The collected sludge was configured with an enrichment culture solution to domesticate anaerobic sludge and enrich it with anaerobic microorganisms. Serum vials of 500 mL were used to domesticate the sludge by adding 100 mL of sludge and 250 mL of enrichment culture solution. The vials were vented with nitrogen for 15 min, and then sealed with a lid to ensure an anaerobic environment. The enrichment solution consisted of 0.36 g per L  $KNO_3$ , 0.21 g per L  $NaHCO_3$ , 0.34 g per L  $KH_2PO_4$ , 0.086 g per L  $NH_4Cl$ , 0.076 g per L  $MgCl_2$ , 0.003 g per L  $CaCl_2$ , and 0.25 mL per L trace element solution.<sup>36</sup> The trace element solution consisted of 0.1 mg per L

$FeSO_4 \cdot 7H_2O$ , 0.03 mg per L  $H_3BO_3$ , 0.036 mg per L  $Na_2MoO_4 \cdot 2H_2O$ , 0.12 mg per L  $MnCl_2 \cdot 2H_2O$ , 0.07 mg per L  $ZnCl_2$ , 0.12 mg per L  $CoCl_2 \cdot 6H_2O$ , 0.024 mg per L  $NiCl_2 \cdot 6H_2O$ , and 0.015 mg per L  $CuSO_4 \cdot 5H_2O$ .<sup>37</sup> The culture was transferred to a new vial and incubated every 5 days.

#### 4.2. Experimental design

Synthetic wastewater was used to simulate  $NO_3^-$ -N contaminated groundwater, and the synthetic wastewater consisted of 0.45 g per L  $KNO_3$ , 0.14 g per L  $KH_2PO_4$ , 0.03 g per L  $MgCl_2$ , 0.001 g per L  $CaCl_2$ , 0.42 g per L  $NaHCO_3$ , and 0.1 mL per L trace element.<sup>36</sup>

In the batch experiments, synthetic groundwater was used to simulate groundwater conditions in the presence of both heavy metals and  $NO_3^-$ -N. For that, 50 mL of synthetic groundwater was added to 100 mL serum bottles. The experimental group with 1 mM  $Mn^{2+}$  and no sludge was added as a blank control (CK), and the experimental group with 2 g of cultured anaerobic sludge without  $Mn^{2+}$  was added as the control group (A). All other experimental groups, that is, B, C, D, E, and F, were added with 2 g of anaerobic sludge, and the initial  $Mn^{2+}$  concentrations were set to 1, 5, 10, 15, and 20 mM  $Mn^{2+}$ , respectively, according to different levels of  $Mn^{2+}$  contamination. The initial pH was adjusted to 7.2. Each serum vial was rinsed with nitrogen for 15 min and then sealed with a cap to ensure an anaerobic environment. Samples were withdrawn at 150 rpm and 30 °C on days 1, 2, 4, 6, 8, 10, and 12 to determine the contents of  $NO_3^-$ -N,  $NO_2^-$ -N,  $NH_4^+$ -N,  $N_2O$ , and  $Mn^{2+}$ . The pH and total nitrogen (TN) content of the supernatant were measured on days 0 and 12. On day 12, the sludge was also collected for 16S rRNA high-throughput sequencing. Three replicates were set for both the treatment and control groups.<sup>36</sup>

#### 4.3. Analysis methods for abiotic indicators

The concentrations of  $NH_4^+$ -N,  $NO_2^-$ -N,  $NO_3^-$ -N, and TN were determined using standard methods.<sup>38</sup>  $NH_4^+$ -N was quantified using indophenol-blue spectrophotometry at 625 nm.  $NO_2^-$ -N was measured using *N*-(1-naphthalene)-diaminoethane spectrophotometry at 540 nm.  $NO_3^-$ -N was assessed using ultraviolet spectrophotometry at 220 and 275 nm. TN was assessed using alkaline potassium persulfate digestion-ultraviolet spectrophotometry at 220 and 275 nm.  $N_2O$  content was determined using gas chromatography.  $Mn^{2+}$  concentration was determined using inductively coupled plasma emission spectrometry. The pH value was determined using a pH meter.

#### 4.4. High-throughput sequencing analysis

After centrifugation of different treatment groups for 12 d, the sludge was placed in 10 mL centrifuge tubes, labelled according to different treatments, and sent to Nanjing Paisenuo Gene Technology Co., Ltd for sequencing. Primers 338F (5'-ACTCC-TACGGGAGGCAGCA-3') and 806R (5'-GGAC-TACHVGGGGTWTCTAAT-3') were used to amplify the V3-V4 region of the bacterial 16S rRNA gene.<sup>39</sup>



#### 4.5. Data processing and analysis

Excel 2016 and Origin 2018 were used for data processing and plotting. SPSS 22.0 was used for the analysis of significance.

### Author contributions

Jiang Zhaojie: experimental design, data analysis and writing – original draft. Huang Xuejiao: resources, methodology and writing – review & editing. Wang Shuangfei: project administration, funding acquisition. Xiong Jianhua: writing – review & editing. Chen Yongli: experimental design and methodology. Xie Chunmin: methodology.

### Conflicts of interest

There are no conflicts to declare.

### Acknowledgements

This project was funded by China Postdoctoral Science Foundation (2022M710850); Technological Innovation Team for Efficient Management of Mariculture Tailwater in Beibu Gulf (GuikeAD23026330); Nanning Innovation and Entrepreneur Leading Talent Project (2021001).

### References

- M. Arauzo, *Sci. Total Environ.*, 2017, **575**, 799–812.
- J. Liu, J. Su, A. Ali, Z. Wang and R. Zhang, *J. Hazard. Mater.*, 2022, **423**, 126976.
- A. Bhatnagar and M. Sillanpää, *Chem. Eng. J.*, 2011, **168**, 493–504.
- Y. Hu, G. Wu, R. Li, L. Xiao and X. Zhan, *Water Res.*, 2020, **179**, 115914.
- G. B. Li, X. Du, H. Yu, Q. Rong, S. Fang and H. Liang, *J. Water Process. Eng.*, 2016, **52**, 9–16.
- J. Wu, Y. Yin and J. Wang, *Int. J. Hydrogen Energy*, 2018, **43**, 1–15.
- X. Luo, C. Peng, P. Shao, A. Tang, A. Huang, Q. Wu, L. Sun, L. Yang, H. Shi and X. Luo, *Environ. Res.*, 2021, **194**, 110744.
- T. Li and Z. P. Li, *BioChem*, 2022, **8**, 131–134.
- D. Jiang and H. B. Yu, *Water Sci. Technol.*, 2016, **42**, 133–136.
- Y. Zong and N. Y. Ji, *Environ. Technol. Innovation*, 2013, **18**, 20.
- P. L. McCarty, *Public Works*, 1964, **95**, 107–112.
- S. I. You, Y. P. Tsai and R. Y. Huang, *Environ. Eng. Sci.*, 2009, **26**, 1207–1215.
- Y. H. Bai, Y. Y. Chang, J. S. Liang, C. Chen and J. H. Qu, *Water Res.*, 2016, **106**, 126–134.
- Y. Wang, Y. H. Bai, J. F. Su, A. Ali, Z. H. Gao, T. L. Huang, M. Cao and M. Q. Ren, *Chem. Eng. J.*, 2023, **461**, 141878.
- T. X. He, D. T. Xie, J. P. Ni, Z. Li and Z. L. Li, *Water*, 2020, **12**, 1701–1712.
- Y. Liu, Y. Wang, X. Song, X. Hou, X. Cao and Y. Wang, *Sci. Total Environ.*, 2023, **899**, 165656.
- Y. H. Bai, J. F. Su, Q. Wen, T. L. Huang, Q. Chang and A. Ali, *J. Hazard. Mater.*, 2021, **408**, 124414.
- X. Wang, G. J. Xie, N. Tian, C. C. Dang, C. Cai, J. Ding, B. F. Liu, D. F. Xing, N. Q. Ren and Q. Wang, *Sci. Total Environ.*, 2022, **822**, 153513.
- L. X. Ai, F. Deng, F. Hu and X. H. Zhang, *Ind. Water Treat.*, 2019, **39**, 69–73.
- J. X. Zuo, J. Z. Hu, Z. Lu and X. S. Gu, *China Biogas*, 1998, **1**, 3–7.
- Y. H. Bai, J. F. Su, A. Ali, Q. Chang, Z. H. Gao, Y. Wang and Y. Liu, *Sci. Total Environ.*, 2022, **810**, 151185.
- D. Swathi, P. C. Sabumon and S. M. Maliyekkal, *Int. Biodeterior. Biodegrad.*, 2017, **119**, 499–510.
- H. Yu and J. R. Leadbetter, *Nature*, 2020, **583**, 453–458.
- I. A. Katsoyiannis and A. I. Zouboulis, *Water Res.*, 2004, **38**, 1922–1932.
- D. Flores-Rentería, A. Rincón, F. Valladares and J. Curiel Yuste, *Soil Biol. Biochem.*, 2016, **92**, 79–90.
- R. Liao, K. Shen, A. M. Li, P. Shi, Y. Li, Q. Shi and Z. Wang, *Bioresour. Technol.*, 2013, **134**, 190–197.
- X. Zhou, Z. Y. Yin, D. L. Ge, G. L. Wang and W. Zhang, *J. Chem. Technol. Biotechnol.*, 2020, **95**, 2229–2236.
- G. Capson-Tojo, R. Moscoviz, D. Ruiz, S. C. Gaëlle, T. Eric, R. Maxime, C. Marion, S. Jean-Philippe, G. Nicolas, D. Jean-Philippe and E. Renaud, *Bioresour. Technol.*, 2018, **260**, 157–168.
- C. Wang, Q. N. Lin, Y. Y. Yao, R. H. Xu, X. S. Wu and F. F. Meng, *Bioresour. Technol.*, 2022, **358**, 127373.
- S. Q. Zhang, Z. Kong, H. Wang, Q. Yan, D. V. Vayenas and G. S. Zhang, *Chem. Eng. J.*, 2022, **433**, 133535.
- J. Y. Zhen, Y. Y. Zhao, X. F. Yu, W. S. Guo, Z. M. Qiao, S. Ismail and S. Q. Ni, *ACS ES&T Water*, 2022, **2**, 1119–1131.
- Y. P. Song, H. Gong, Q. Yuan, F. M. Chang, J. B. Wang and W. Kaijun, *J. Environ. Sci.*, 2021, **41**, 70–82.
- X. Xin, B. X. Li, X. Liu, W. Y. Yang and Q. Liu, *J. Environ. Manage.*, 2023, **331**, 117298.
- X. K. Li, C. K. Liu, H. W. Xie, Y. J. Sun, S. W. Xu and G. G. Liu, *Chemosphere*, 2023, **320**, 138097.
- Y. Y. Shi, H. X. Ming, Q. R. Chen, Y. Yu and J. F. Fan, *Microbiol. Bull.*, 2021, **48**, 2895–2901.
- Y. M. Pang and J. L. Wang, *Bioresour. Technol.*, 2021, **342**, 125960.
- Y. M. Pang, J. L. Wang, S. J. Li and G. D. Ji, *ACS ES&T Water*, 2021, **1**, 1566–1576.
- State Environmental Protection Administration of China, *Water and Wastewater Analysis Methods*, China Environmental Science Press, Beijing, China, 2002, pp. 132–286.
- Y. M. Pang and J. L. Wang, *Bioresour. Technol.*, 2020, **318**, 124105.

